

## Supporting Information

### [Ga@Bi<sub>10</sub>(NbMes)<sub>2</sub>]<sup>3-</sup>: A Linear Nb-Ga<sup>I</sup>-Nb Filament Coordinated by A Bismuth Cage

Lei Qiao<sup>a</sup>, Tao Yang<sup>b\*</sup>, Gernot Frenking<sup>c,d</sup>, and Zhong-Ming Sun<sup>a\*</sup>

<sup>a</sup> State Key Laboratory of Element-Organic Chemistry, Tianjin Key Lab for Institution Rare Earth Materials and Applications, School of Materials Science and Engineering, Nankai University, Tianjin 300350, Tianjin, China

<sup>b</sup> MOE Key Laboratory for Non-Equilibrium Synthesis and Modulation of Condensed Matter, School of Physics, Xi'an Jiaotong University, Xi'an 710049, Shaanxi, China

<sup>c</sup> Donostia International Physics Center (DIPC), P.K. 1072, 20080 Donostia, Euskadi, Spain

<sup>d</sup> Fachbereich Chemie, Philipps-Universität Marburg, Hans-Meerwein-Strasse 4, 35043 Marburg, Germany

#### Content

1. Experimental Procedures .....	2
1.1 Synthesis of [K(2.2.2-crypt)] <sub>3</sub> [Ga@Bi <sub>10</sub> (NbMes) <sub>2</sub> ]: .....	2
1.2 X-ray Diffraction: .....	2
1.3 Electrospray Ionization Mass Spectrometry (ESI-MS) Investigations: .....	2
1.4 Energy Dispersive X-ray (EDX): .....	2
1.5 Quantum chemical methods: .....	2
2. Results and Discussion .....	3
2.1 Crystallographic Supplementation: .....	3
2.2 ESI-MS studies: .....	5
2.3 Energy dispersive X-ray (EDX) spectroscopic analysis: .....	7
2.4 Computational results: .....	8
2.4.1 Structural Optimization of [Ga@Bi <sub>10</sub> (NbMes) <sub>2</sub> ] <sup>3-</sup> .....	8
2.4.2 LMOs analysis of the anion [Ga@Bi <sub>10</sub> (NbMes) <sub>2</sub> ] <sup>3-</sup> .....	8
2.4.3 Canonical Molecular Orbital (CMO), NPA, bond order, and NLMO analysis of the anion [Ga@Bi <sub>10</sub> (NbMes) <sub>2</sub> ] <sup>3-</sup> .....	13
2.4.4 QTAIM analysis of the anion [Ga@Bi <sub>10</sub> (NbMes) <sub>2</sub> ] <sup>3-</sup> .....	14
2.4.5 EDA-NOCV analysis of the anion [Ga@Bi <sub>10</sub> (NbMes) <sub>2</sub> ] <sup>3-</sup> .....	14
References.....	20

## 1. Experimental Procedures

All manipulations and reactions were performed under a nitrogen atmosphere using standard Schlenk or glovebox techniques. Ethylenediamine (en) (Aldrich, 99%) was freshly distilled by  $\text{CaH}_2$  prior to use. Toluene (Energy Chemical, 99.8%) was distilled from sodium/benzophenone under nitrogen and stored under nitrogen. 2,2,2-crypt (4,7,13,16,21,24-Hexaoxa-1,10-diazabicyclo (8.8.8) hexacosane, purchased from Sigma-Aldrich, 98%, was dried in vacuum for 20 h prior to use. The ternary mixture with a nominal composition of “ $\text{K}_5\text{Ga}_2\text{Bi}_4$ ” was synthesized by heating a stoichiometric mixture of the elements (K: +99%, Ga: 99.9999%, Bi: 99.99% all from Aladdin) at a rate of 100 °C per hour to 800 °C and keeping it for 20 hours in sealed niobium containers closed in evacuated quartz ampules. The furnace was slowly cooled to room temperature at a rate of 100 °C per hour.  $\text{NbMes}_2$  was synthesized according to the reported literature.<sup>[1]</sup>

### 1.1 Synthesis of $[\text{K}(2,2,2\text{-crypt})]_3[\text{Ga@Bi}_{10}(\text{NbMes})_2]$ :

$\text{K}_5\text{Ga}_2\text{Bi}_4$  (117 mg, 0.1 mmol) and 2,2,2-crypt (100mg, 0.26 mmol) were weighed into a 10 mL vial inside a glovebox and dissolved in en (2.5 mL). After stirring for 0.5 hour, the resulting dark blue solution was filtered onto another vial of  $\text{NbMes}_2$  (17 mg, 0.05 mmol) allowed to stir for a further two hours at room temperature. The resulting brown solution was filtered through glass wool and transferred to a test tube, then carefully layered with toluene (3 mL) to allow for crystallization. Small black plate-like crystals of  $[\text{K}(2,2,2\text{-crypt})]_3[\text{Ga@Bi}_{10}(\text{NbMes})_2]$  were isolated after one week in approximately 21% yield in total (based on precursor  $\text{NbMes}_2$  used).

### 1.2 X-ray Diffraction:

Suitable single crystals were selected for X-ray diffraction analyses. Crystallographic data were collected on Rigaku XtalAB Pro MM007 DW diffractometer with graphite monochromated Cu K $\alpha$  radiation ( $\lambda = 1.54184 \text{ \AA}$ ). Structure was solved using direct methods and then refined using SHELXL-2014 and Olex2<sup>2-4</sup> to convergence, in which all the non-hydrogen atoms were refined anisotropically during the final cycles. All hydrogen atoms of the organic molecule were placed by geometrical considerations and were added to the structure factor calculation. We used the PLATON SQUEEZE procedure<sup>[5]</sup> to remove the toluene molecule which could not be modeled properly. A summary of the crystallographic data for the title compound was listed in Table S1. CCDC entry 2162329 for compound **1** contains the supplementary crystallographic data for this paper. These data can be obtained free of charge from the Cambridge Crystallographic Data Centre ([www.ccdc.cam.ac.uk/data\\_request/cif](http://www.ccdc.cam.ac.uk/data_request/cif)).

### 1.3 Electrospray Ionization Mass Spectrometry (ESI-MS) Investigations:

Negative ion mode ESI-MS of the acetonitrile solution of the single crystal of  $[\text{K}(2,2,2\text{-crypt})]_3[\text{Ga@Bi}_{10}(\text{NbMes})_2]$  was measured on an LTQ linear ion trap spectrometer by Agilent Technologies ESI-TOF-MS (6230). The spray voltage was 5.48 kV and the capillary temperature was kept at 300 °C. The capillary voltage was 30 V. The sample was made up inside a glovebox under a nitrogen atmosphere and rapidly transferred to the spectrometer in an airtight syringe by direct infusion with a Harvard syringe pump at 0.2 mL/ min.

### 1.4 Energy Dispersive X-ray (EDX):

EDX analysis on the title cluster was performed using a scanning electron microscope (FE-SEM, JEOL JSM-7800F, Japan). Data acquisition was performed with an acceleration voltage of 15 kV and an accumulation time of 60 s.

### 1.5 Quantum chemical methods:

All calculations described in this paper were performed with the GAUSSIAN 09 program package<sup>[6]</sup>, NBO 6.0 program<sup>[7]</sup>, and ADF2019<sup>[8]</sup>. The geometry optimization and vibrational frequency of the title cluster were performed using the PBE0 functional<sup>[9-10]</sup> and def2-TZVP basis set<sup>[11]</sup>. The confining effect of cations in the solid-state was simulated by using a polarizable continuum model (PCM)<sup>[12]</sup> with a dielectric constant of  $\epsilon_r$ (ethylenediamine)=12.9. The localized molecular orbitals were calculated using the method of Boys and Foster<sup>[13-14]</sup> with Multiwfn 3.7 program<sup>[15]</sup> (Amplitudes in **Figure 2** in the main document are drawn at  $\pm 0.03$  a.u., the thresholds for determining one-center and two-center LMOs are set to 0.85 and 0.7, respectively) and were created with VMD program<sup>[16]</sup>. Quantum theory of atoms in molecules (QTAIM) analysis<sup>[17]</sup> was also performed with Multiwfn 3.7 program. Charges and energies were calculated using NBO 6.0 program.

The bonding situations were analyzed by means of an energy decomposition analysis (EDA)<sup>[18]</sup> together with the natural orbitals for chemical valence (NOCV)<sup>[19]</sup>. The EDA-NOCV calculations<sup>[20]</sup> were carried out with the program package ADF2019 at the BP86(D3)<sup>[21-23]</sup>/TZ2P<sup>[24]</sup> level using the PBE0/def2-TZVP optimized geometries. There are three reasons why the BP86(D3)/TZ2P was employed for EDA-NOCV calculations. First, it has been found previously that the functional has only slightly influence on EDA-NOCV results.<sup>[25,26]</sup> Second, our previous calculation results reveal that the BP86-D3 functional could give reliable EDA-NOCV results for Zintl clusters.<sup>[27,28]</sup> Third, BP86-D3 that belongs to GGA is obviously less time-consuming than those hybrid functionals like PBE0 in ADF. For the basis set, def2-TZVP is no available in ADF software while the TZ2P basis set in ADF software is as large as def2-TZVP.

## 2. Results and Discussion

### 2.1 Crystallographic Supplementation:

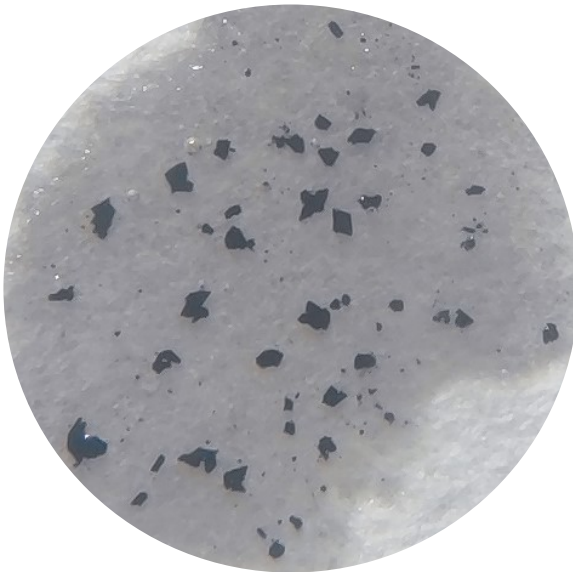


**Figure S1.** Crystals of  $[\text{K}(2.2.2\text{-crypt})_3\text{[Ga@Bi}_{10}\text{(NbMes)}_2\text{]}]$ . (1) dispersed silicon oil.

**Table S1.** X-ray measurements and structure solutions of  $[\text{K}(2.2.2\text{-crypt})_3\text{[Ga@Bi}_{10}\text{(NbMes)}_2\text{]}}$ .

Compound	<b>1</b>
Empirical formula	$\text{C}_{79}\text{H}_{140}\text{N}_6\text{O}_{18}\text{K}_3\text{Nb}_2\text{Bi}_{10}\text{Ga}$
Formula weight	3924.60
Crystal system	Triclinic
Space group	<i>P</i> 1
<i>a</i> / Å	13.0159(3)
<i>b</i> / Å	15.5134(4)
<i>c</i> / Å	27.2898(8)
$\alpha/^\circ$	89.942(2)
$\beta/^\circ$	86.298(2)
$\gamma/^\circ$	76.288(2)
<i>V</i> / Å <sup>3</sup>	5341.6(2)
<i>Z</i>	2
$\rho_{\text{calc}}/\text{g}\cdot\text{cm}^{-3}$	2.440
$\mu(\text{Cu}_{\text{K}\alpha})/\text{mm}^{-1}$	35.072
<i>F</i> (000)	3600
2 <i>θ</i> range / °	7.006 to 151.974
Reflections collected / unique	58304/27556
Data / restraints / parameters	27556/6510/2194
<i>R</i> <sub>1</sub> /w <i>R</i> <sub>2</sub> ( <i>I</i> >2σ( <i>I</i> )) <sup>a</sup>	0.0516; 0.1172
<i>R</i> <sub>1</sub> /w <i>R</i> <sub>2</sub> (all data)	0.0618; 0.1236
<i>GooF</i> (all data) <sup>b</sup>	1.026
Data completeness	1.24/0.62

Max. peak/hole /e <sup>-</sup> ·Å <sup>-3</sup>	2.07/-1.85
---	------------

$$^a R_1 = \sum ||F_o - |F_c|| / \sum |F_o|; wR_2 = \{ \sum w[(F_o)^2 - (F_c)^2]^2 / \sum w[(F_o)^2]^2 \}^{1/2}$$

$$^b Goof = \{ \sum w[(F_o)^2 - (F_c)^2]^2 / (n-p) \}^{1/2}$$

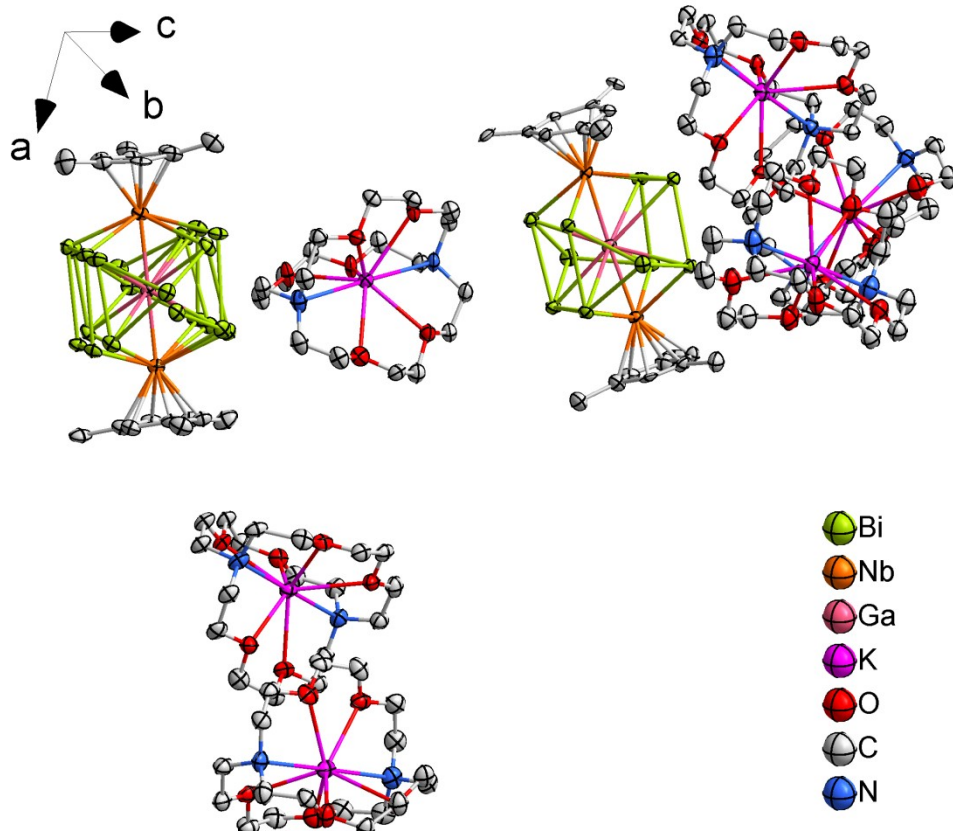


**Figure S2.** The molecular structure of **1** (thermal ellipsoids are drawn at 50% probability). The minor components are omitted for clarity.

The asymmetric cell contains two anionic clusters  $[\text{Ga}@\text{Bi}_{10}(\text{NbMes})_2]^{3-}$  in different sites. Site 1 appears to be well-behaved, however, site 2 is slightly disordered. Positions of disordered atoms are given in semitransparent mode in Figure S3. Thermal ellipsoids are drawn at 50% probability.

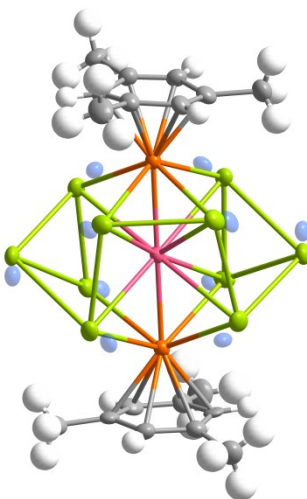


**Figure S3.** The molecular structure of **1** (thermal ellipsoids are drawn at 50% probability). Positions of disordered atoms are given in semitransparent mode.

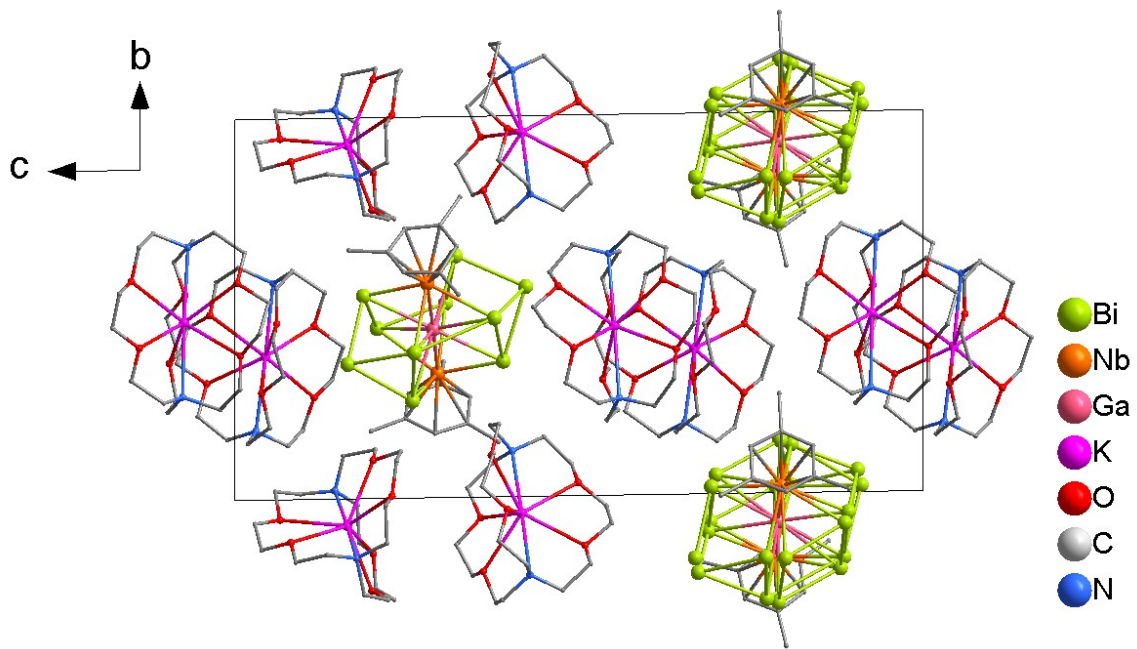


**Figure S4.** The unit cell of compound 1. Minor components in the structure are omitted for clarity.

## 2.2 ESI-MS studies:

The ESI-MS of the acetonitrile solution of the crystals of  $[K(2.2.2\text{-crypt})_3][Ga@Bi_{10}(NbMes)_2]$  (Figure 5(a)) shows a parent peak corresponding to  $[Bi_{10}GaNb_2Mes_2]^-$  ( $m/z=2584.7237$ ) along with other peaks, such as  $[Bi_5Nb_2Mes_2]^-$  ( $m/z=1470.9004$ ),  $[Bi_5NbMes]^-$  ( $m/z=1257.8884$ ),  $[Bi_5O_2]^-$  ( $m/z=1076.8886$ ),  $[Bi_5]^-$  ( $m/z=1044.8927$ ),  $[Bi_7]^-$  ( $m/z=1462.8494$ ),  $[Bi_{11}]^-$  ( $m/z=2298.7617$ ),  $[Bi_{13}]^-$  ( $m/z=2716.7237$ ). Measured and simulated isotope distributions for all species are shown in the Figures S5-S10.

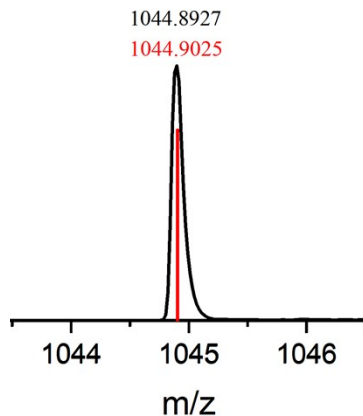


**Figure S5.** Measured (top) and simulated (bottom) spectrum of the fragment  $[Bi_5]^-$ .

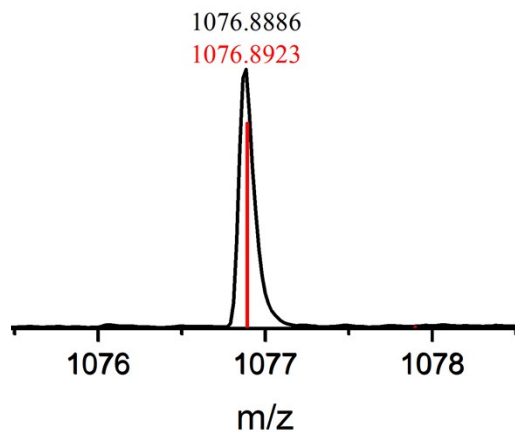


Figure S6. Measured (top) and simulated (bottom) spectrum of the fragment  $[\text{Bi}_5\text{O}_2]^-$ .

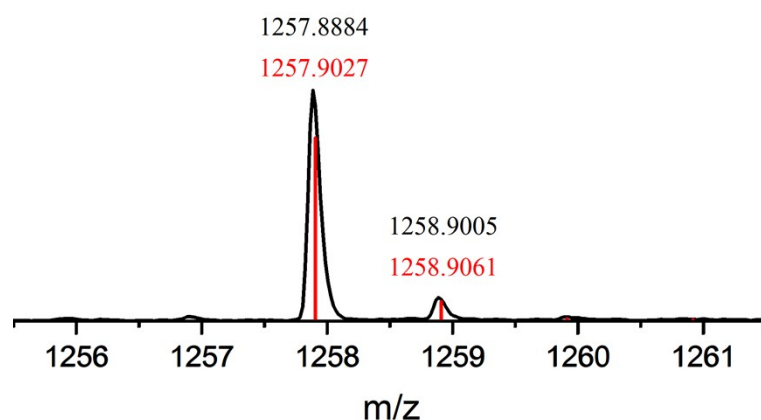


Figure S7. Measured (top) and simulated (bottom) spectrum of the fragment  $[\text{Bi}_5\text{NbMes}]^-$ .

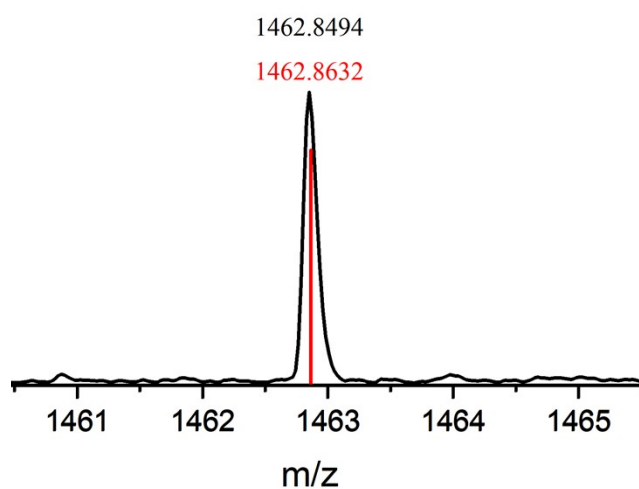
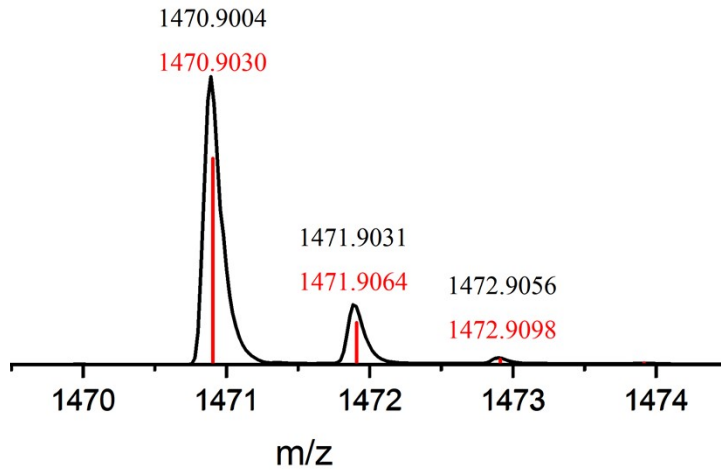
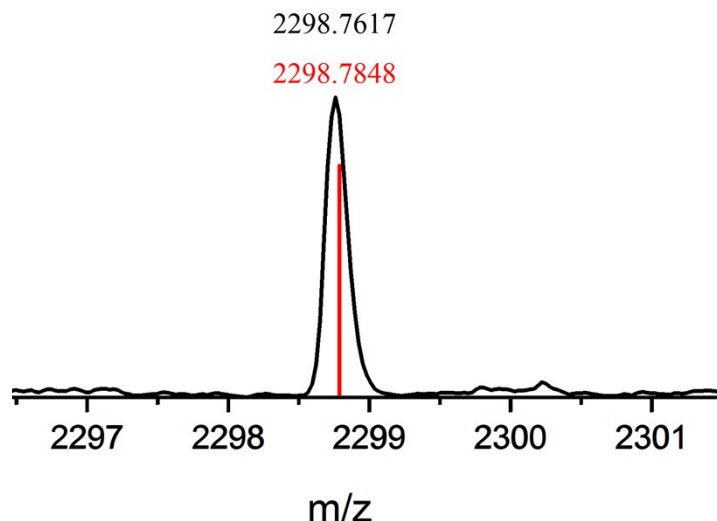


Figure S8. Measured (top) and simulated (bottom) spectrum of the fragment  $[\text{Bi}_7]^-$ .

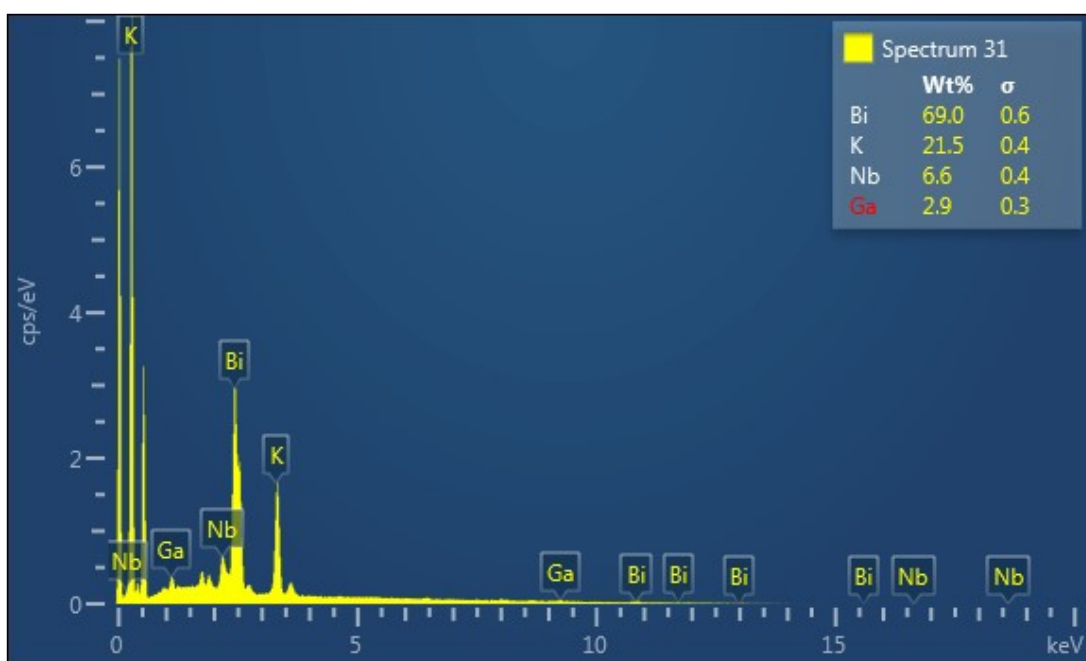


**Figure S9.** Measured (top) and simulated (bottom) spectrum of the fragment  $[\text{Bi}_5\text{Nb}_2\text{Mes}_2]^-$ .



**Figure S10.** Measured (top) and simulated (bottom) spectrum of the fragment  $[\text{Bi}_{11}]^-$ .

### 2.3 Energy dispersive X-ray (EDX) spectroscopic analysis:



Element	Element wt %	Atom %	Element ratio (exp.)	Element ratio (calc.)
Bi	69.0	33.0	10.0	10.0
Nb	6.6	7.1	2.2	2.0
Ga	2.9	4.2	1.3	1.0
K	21.5	55.0	16.7	3.0

The deviation of the experimental K content from the calculated is a relatively common phenomenon for this class of compounds, however, which does not affect the ratios of the other elements (as shown in the table).

Figure S11. EDX analysis of **1** (K, Ga, Nb, and Bi).

## 2.4 Computational results:

### 2.4.1 Structural Optimization of $[\text{Ga}@\text{Bi}_{10}(\text{NbMes})_2]^{3-}$

Table S2. Selected bond lengths (in Å) of the experiment and optimized geometries of  $[\text{Ga}@\text{Bi}_{10}(\text{NbMes})_2]^{3-}$  at the PBE0/def2-tzvp level of theory.

	Experimental	Theoretical
Bi1-Bi2	3.0613(7)	3.04767
Bi1-Bi3	2.9599(8)	2.93081
Bi2-Bi8	3.0016(6)	3.01251
Bi8-Bi7	3.0395(7)	3.01588
Bi7-Bi6	3.0527(7)	3.05270
Bi6-Bi8	3.0877(8)	3.05185
Bi3-Bi13	3.0424(7)	3.03781
Bi13-Bi12	3.0343(7)	3.01588
Bi12-Bi9	3.0350(7)	3.01863
Bi9-Bi11	3.0810(7)	3.05022
Bi11-Bi12	3.0892(7)	3.04518
Nb4-Bi1	3.0104(11)	3.01453
Nb4-Bi3	2.9697(9)	3.00669
Nb4-Bi11	2.9839(12)	2.97357
Nb4-Bi6	2.9421(10)	2.97115
Nb10-Bi2	3.0048(12)	3.03088
Nb10-Bi7	2.9902(10)	3.01227
Nb10-Bi9	2.9979(12)	3.01443
Nb10-Bi13	2.9626(10)	3.00881
Nb4-Ga5	2.6599(20)	2.65211
Ga5-Nb10	2.6408(20)	2.63922

### 2.4.2 LMOs analysis of the anion $[\text{Ga}@\text{Bi}_{10}(\text{NbMes})_2]^{3-}$

The bonding situation in the title cluster  $[\text{Ga}@\text{Bi}_{10}(\text{NbMes})_2]^{3-}$  was analyzed by the localized molecular orbitals using the method of Boys and Foster. Table S3 gives an overview of all LMOs that are directly involved in the cluster bonding and the types of bonds. Furthermore, one lone pair at each Bi atom was found (Figure S12). Eleven 2c2e Bi-Bi bonds (Figure S13) and seven 2c2e Nb-Bi bonds (Figure S14) between each Nb atom and the neighboring Bi atoms are present. The two Nb-Ga bonds are mainly covalent (Figure S15A and S15B).

**Table S3.** All of the localized molecular orbitals of the cluster  $[Ga@Bi_{10}(NbMes)_2]^{3-}$  are directly involved in the bonding of Bi, Nb, and Ga atoms.

Localized Molecular Orbitals	Type	atoms	Contributions	Figure
145	Lone pair	8	95.6%	S12A
148		12	96.0%	S12B
149		3	90.3%	S12C
152		2	89.7%	S12D
55		13	90.3%	S12E
154		9	88.6%	S12F
28		6	90.8%	S12G
29		11	91.0%	S12H
60		7	92.8%	S12I
160		1	93.5%	S12J
1	2c-2e Bi-Bi bond	12-13	50.0%, 40.4%	S13A
3		9-12	40.1%, 49.3%	S13B
192		3-13	42.6%, 41.8%	S13C
193		2-8	41.5%, 49.6%	S13D
194		11-12	38.4%, 50.7%	S13E
195		6-8	37.1%, 51.3%	S13F
197		7-8	40.4%, 49.0%	S13G
202		1-3	46.4%, 43.4%	S13H
203		6-7	40.2%, 43.6%	S13I
204		1-2	43.7%, 41.7%	S13J
209	2c-2e Nb-Bi bond	9-11	42.5%, 41.5%	S13K
2		10-13	22.4%, 59.2%	S14A
191		4-11	21.4%, 60.1%	S14B
196		7-10	58.0%, 22.8%	S14C
200		4-6	22.2%, 57.5%	S14D
205		9-10	57.1%, 23.0%	S14E
206		2-10	57.3%, 22.9%	S14F
211		1-4	55.4%, 23.4%	S14G
201	2c-2e Nb-Ga bond	3-4	57.1%, 23.0%	S14H
208		10-5	37.0%, 36.0%	S15A
210		4-5	37.8%, 35.3%	S15B

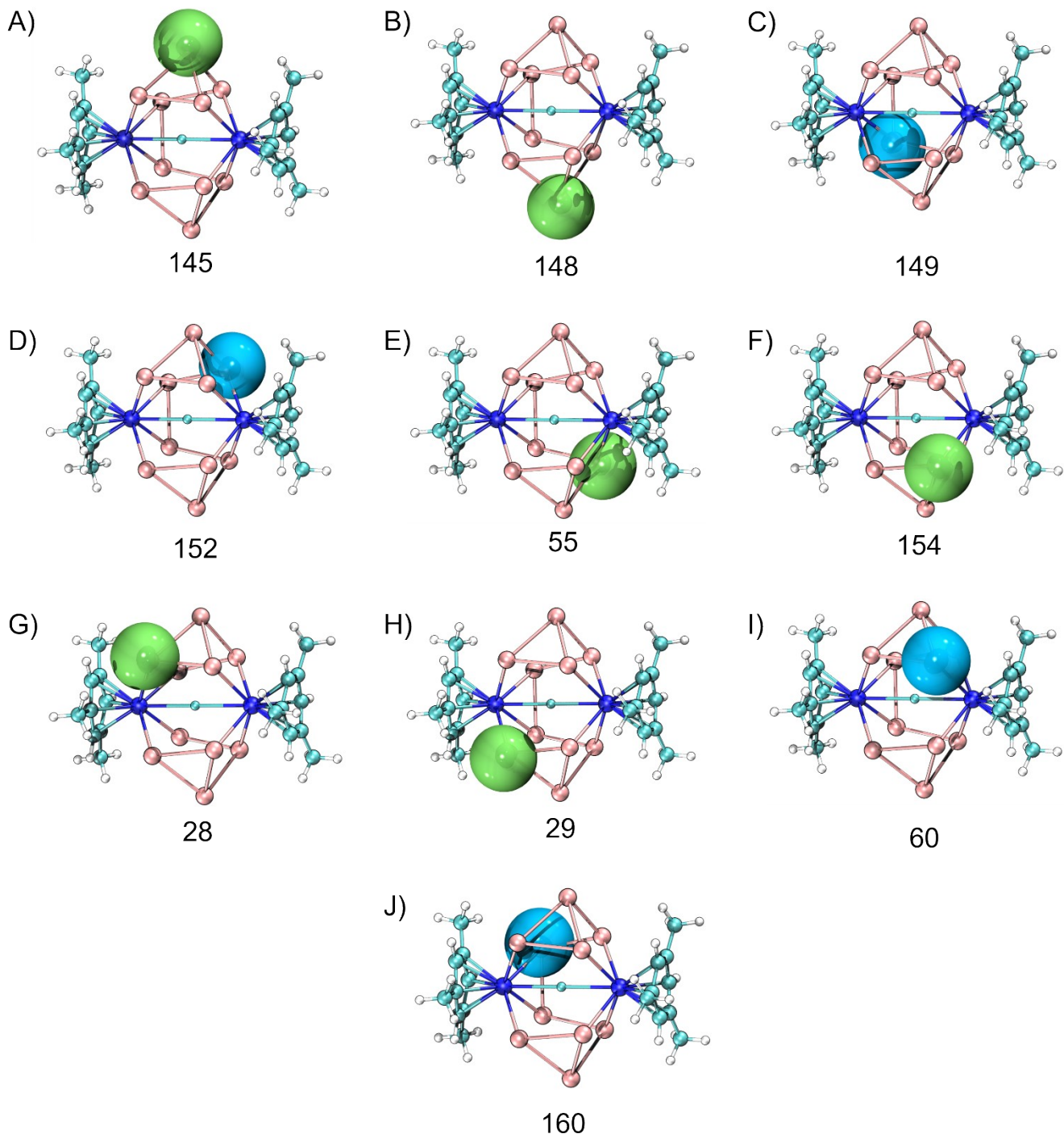


**Figure S12.** Localized molecular orbitals of  $[\text{Ga}@\text{Bi}_{10}(\text{NbMes})_2]^{3-}$  that are lone pairs on ten Bi atoms. Amplitudes are drawn at 0.03 a.u..

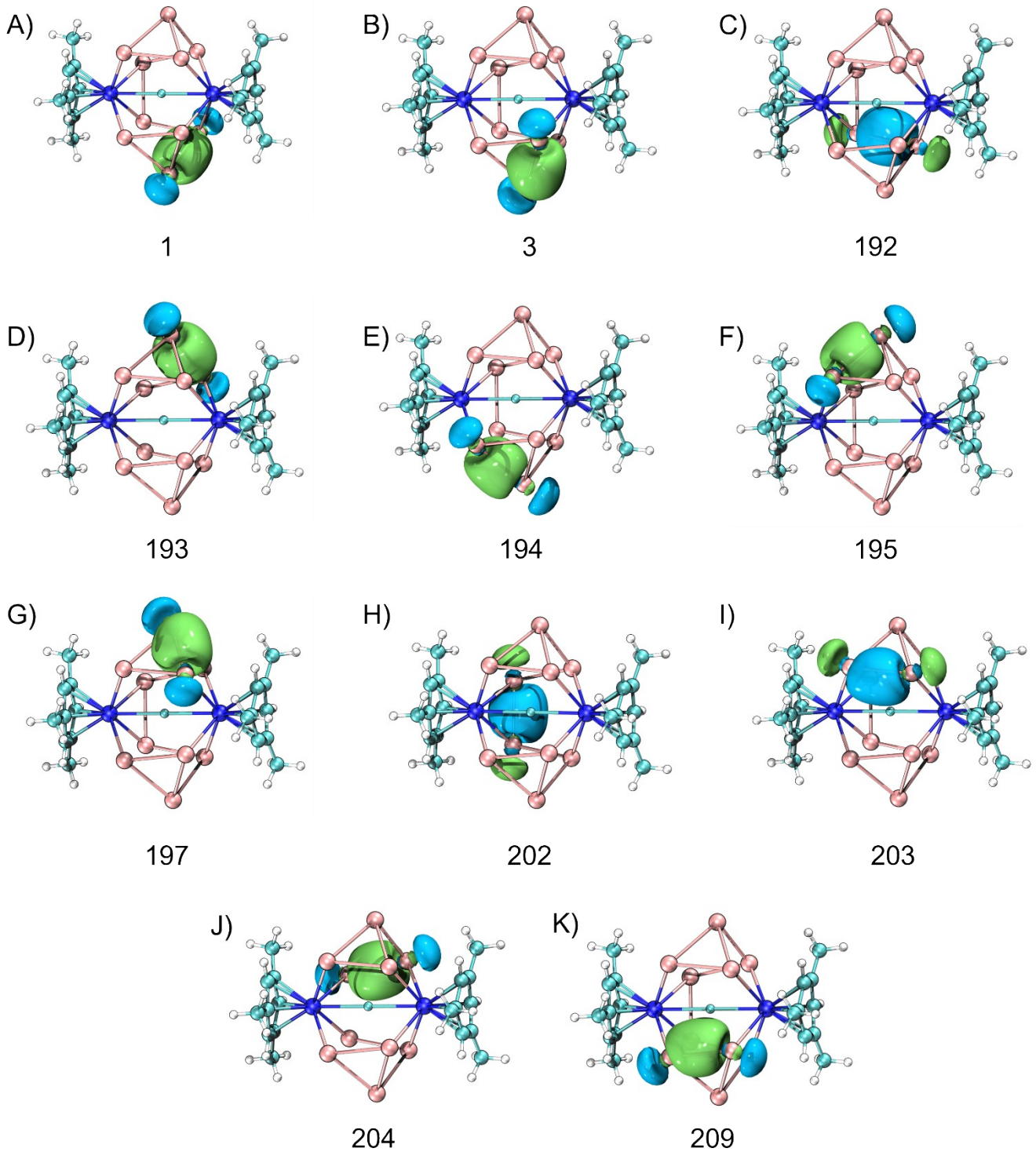


**Figure S13.** Localized molecular orbitals of  $[\text{Ga}@\text{Bi}_{10}(\text{NbMes})_2]^{3-}$  that are 2c-2e Bi-Bi bonds. Amplitudes are drawn at 0.03 a.u..

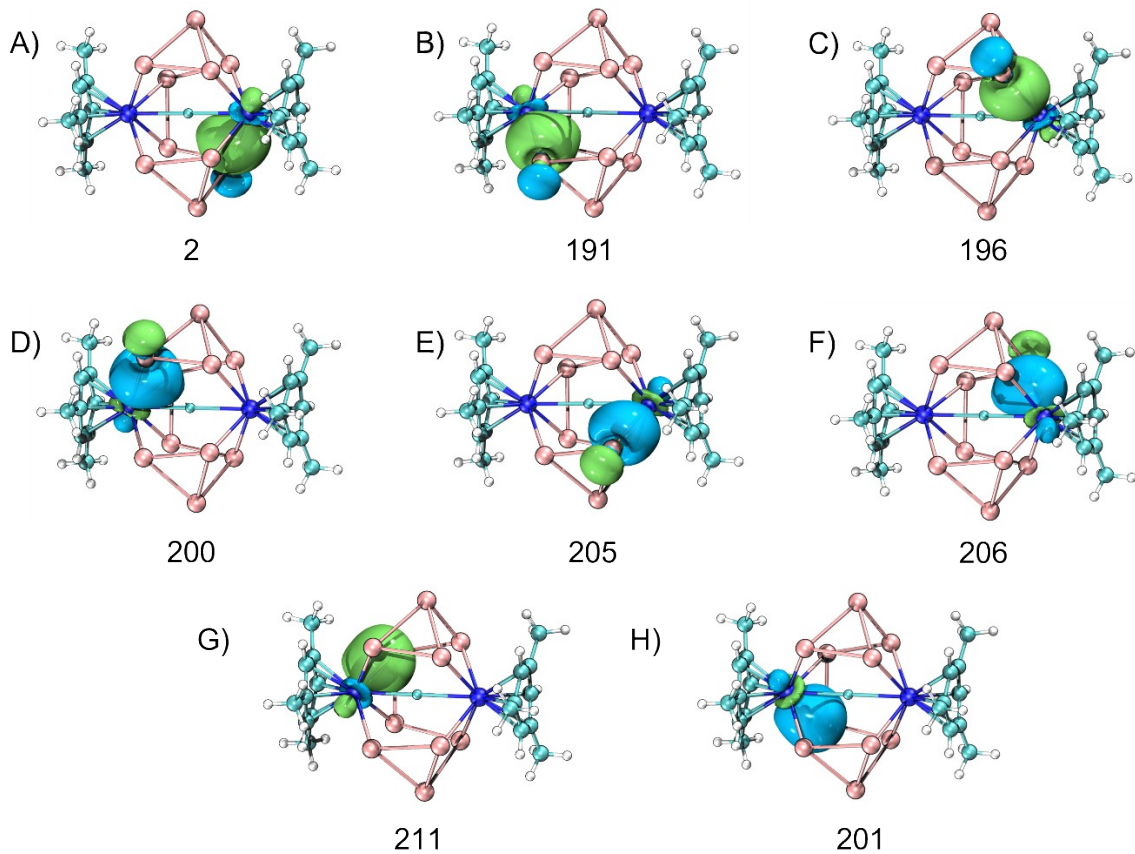


**Figure S14.** Localized molecular orbitals of  $[\text{Ga}@\text{Bi}_{10}(\text{NbMes})_2]^{3-}$  that are 2c-2e Nb-Bi bonds. Amplitudes are drawn at 0.03 a.u..

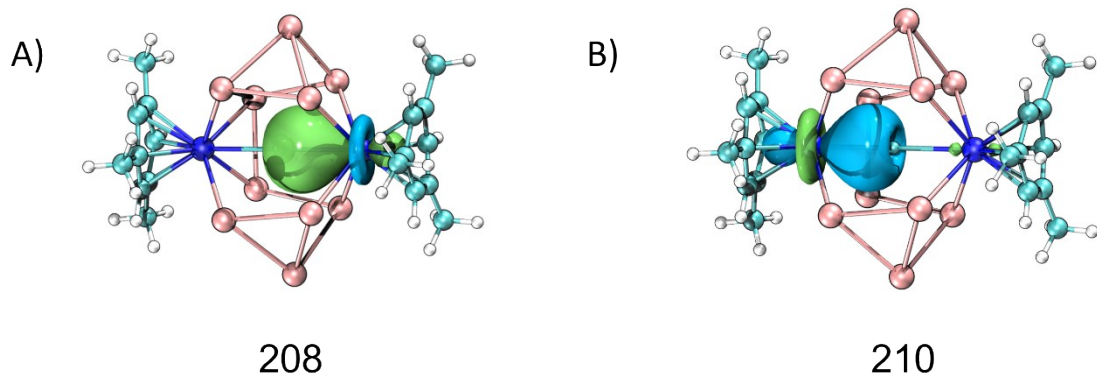


**Figure S15.** Localized molecular orbitals of  $[\text{Ga}@\text{Bi}_{10}(\text{NbMes})_2]^{3-}$  that are 2c-2e Nb-Ga covalent bonds. Amplitudes are drawn at 0.03 a.u..

### 2.4.3 Canonical Molecular Orbital (CMO), NPA, bond order, and NLMO analysis of the anion $[\text{Ga}@\text{Bi}_{10}(\text{NbMes})_2]^{3-}$

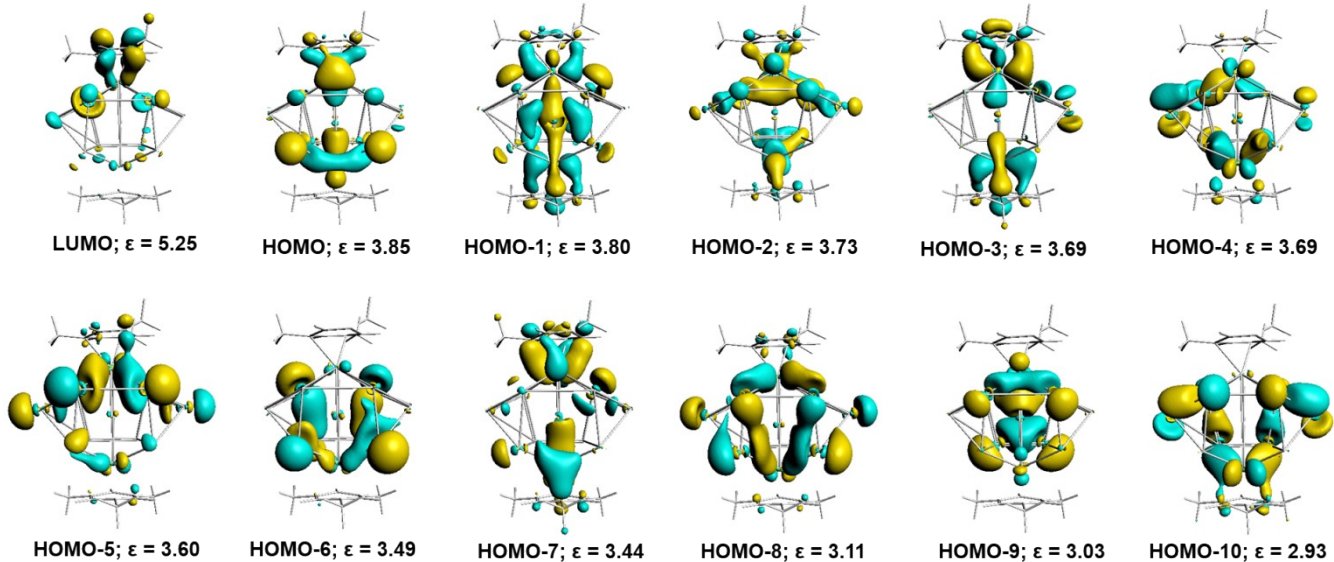


Figure S16. Representative molecular orbitals of the title cluster were shown. The interactions between the central Ga atom and two Nb atoms can be found in HOMO, HOMO-1, HOMO-3, and HOMO-7 orbitals. Amplitudes are drawn at 0.03 a.u..

Table S4. Natural charges (q), Wiberg bond order (P), and the composition analysis of Ga-Nb bonds of the title cluster with NBO6.0.

Bond	q(Ga)	q(Nb)	Occupied number	Ga-Nb bond composition	Wiberg bond order
Ga5-Nb4	+0.23	-0.35	1.64	51% Ga ( $s^{50\%}p^{50\%}$ ) + 49% Nb ( $s^{32\%}d^{68\%}$ )	0.66
Ga5-Nb10	+0.23	-0.39	1.64	51% Ga ( $s^{50\%}p^{50\%}$ ) + 49% Nb ( $s^{32\%}d^{68\%}$ )	0.66

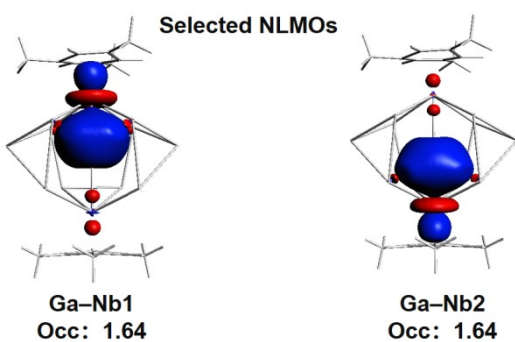
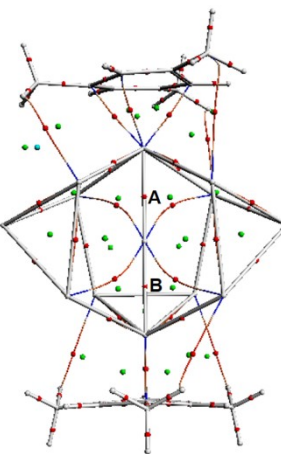


Figure S17. Representative natural localized molecular orbitals of the title cluster were shown. Amplitudes are drawn at 0.03 a.u..

#### 2.4.4 QTAIM analysis of the anion $[\text{Ga}@\text{Bi}_{10}(\text{NbMes})_2]^{3-}$



	A	B
Density of all electrons	0.0592	0.0593
Potential energy density $V(r)$	-0.0422	-0.0434
Laplacian of electron density	$-0.42 \times 10^{-3}$	$0.37 \times 10^{-2}$
Energy density $E(r)$ or $H(r)$	-0.0212	-0.0213
$ V(\text{BCP}) /G(\text{BCP})$	2.01	1.96
$H(\text{BCP})/\rho(\text{BCP})$	-0.3581	-0.3591
$\eta$ index	0.5082	0.4812

**Figure S18.** Atoms-in-Molecule analysis of the title cluster. (a) Red dots are bond critical points, green dots are ring critical points, and blue dots are cage critical points. The parameters were listed in the following table. (b) Plot of the Laplacian  $\nabla^2\rho(r)$  of Nb-Ga-Nb planes. Green dashed lines indicate areas of charge concentration ( $\nabla^2\rho(r)<0$ ) while solid purple lines show areas of charge depletion ( $\nabla^2\rho(r)>0$ ).

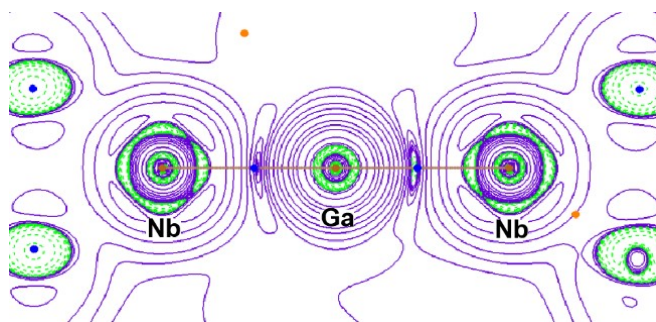
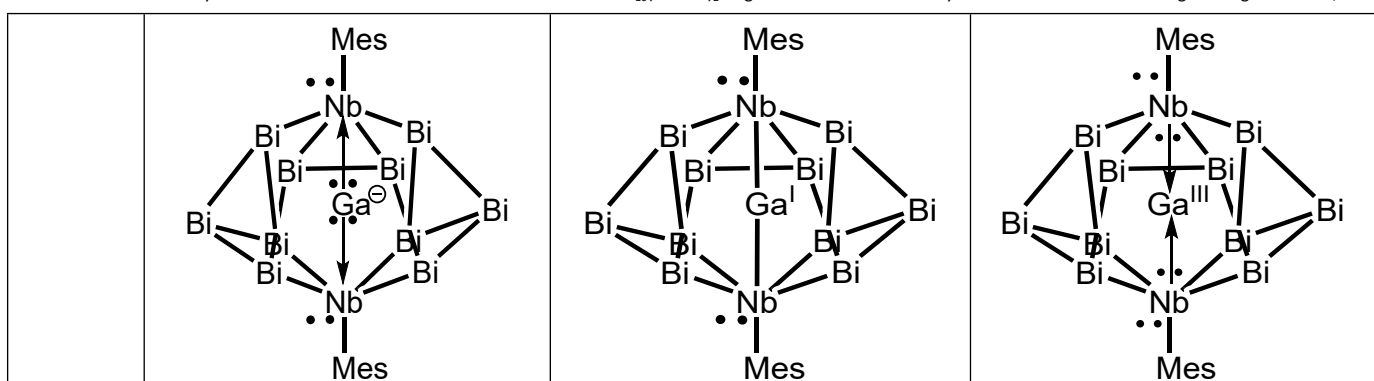


**Figure S19.** Plot of the Laplacian  $\nabla^2\rho(r)$  of Nb-Ga-Nb planes. Green dashed lines indicate areas of charge concentration ( $\nabla^2\rho(r)<0$ ) while solid purple lines show areas of charge depletion ( $\nabla^2\rho(r)>0$ ).

#### 2.4.5 EDA-NOCV analysis of the anion $[\text{Ga}@\text{Bi}_{10}(\text{NbMes})_2]^{3-}$

**Table S5.** The analysis of the interaction between the central ion and the  $\text{Bi}_{10}(\text{NbMes})_2$  fragment in the title cluster by the EDA-NOCV method. Energies are given in kcal/mol.



	Ga <sup>-</sup> (singlet) + [Bi <sub>10</sub> Nb <sub>2</sub> Mes <sub>2</sub> ] <sup>2-</sup> (singlet)	Ga <sup>+</sup> (triplet) + [Bi <sub>10</sub> Nb <sub>2</sub> Mes <sub>2</sub> ] <sup>4-</sup> (triplet)	Ga <sup>3+</sup> (singlet) + [Bi <sub>10</sub> Nb <sub>2</sub> Mes <sub>2</sub> ] <sup>6-</sup> (singlet)
ΔE <sub>int</sub>	-64.2	-549.1	-2049.5
ΔE <sub>Pauli</sub>	1034.7	327.4	113.3
ΔE <sub>disp</sub>	-22.2	-22.2	-22.2
ΔE <sub>elstat</sub> <sup>[a]</sup>	-734.9 (68.3%)	-531.0(62.1%)	-1163.4 (54.3%)
ΔE <sub>orb</sub> <sup>[a]</sup>	-341.8 (31.7%)	-323.4(37.9%)	-977.3 (45.7%)

	Ga <sup>+</sup> (triplet) + [Bi <sub>10</sub> Nb <sub>2</sub> Mes <sub>2</sub> ] <sup>4-</sup> (triplet)	
ΔE <sub>int</sub>	-549.1	
ΔE <sub>Pauli</sub>	327.4	
ΔE <sub>disp</sub>	-22.2	
ΔE <sub>elstat</sub> <sup>[a]</sup>	-531.0(62.1%)	
ΔE <sub>orb</sub> <sup>[a]</sup>	-323.4(37.9%)	
ΔE <sub>orb(1)</sub> <sup>[b]</sup>	Nb—Ga(+,+)—Nb electron-sharing bond -111.0(34.3%)	Figure 3
ΔE <sub>orb(2)</sub> <sup>[b]</sup>	Nb—Ga(+,-)—Nb electron-sharing bond -86.5(26.7%)	Figure 3
ΔE <sub>orb(3)</sub> <sup>[b]</sup>	π <sub>⊥</sub> back-donations -42.9(13.3%)	Figure 3
ΔE <sub>orb(4)</sub> <sup>[b]</sup>	π <sub>  </sub> back-donations -40.5(12.5%)	Figure 3
ΔE <sub>orb(rest)</sub> <sup>[b]</sup>	-42.5(13.1%)	

[a]The percentage values in parentheses give the contribution to the total attractive interactions ΔE<sub>elstat</sub> + ΔE<sub>orb</sub>.

[b]The percentage values in parentheses give the contribution to the total orbital interactions ΔE<sub>orb</sub>.

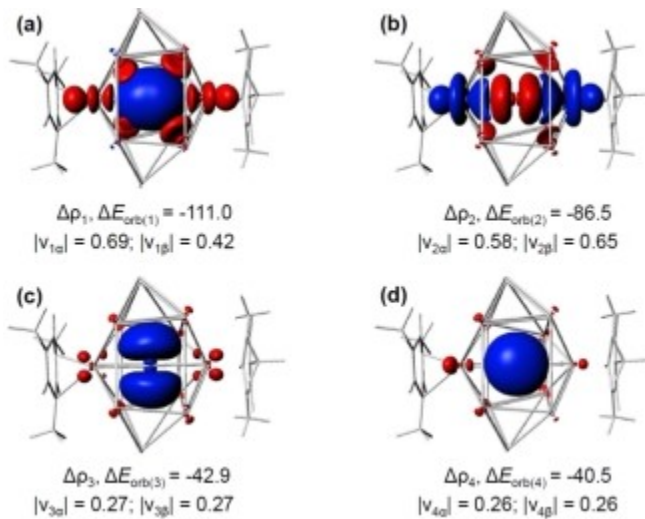


**Figure S20.** Plots of the deformation densities  $\Delta\rho_{1-4}$  (isovalue=0.001) of the most important pairwise orbital interactions in **1a** using Ga<sup>+</sup> (triplet) and [Bi<sub>10</sub>Nb<sub>2</sub>Mes<sub>2</sub>]<sup>4-</sup> (triplet) as interacting fragments with the associated interaction energies (kcal/mol) and their energy eigenvalues v (in e). The charge flow is from red to blue.

**Table S6.** The analysis of the interaction between the central ion Ga and the [Ru<sub>2</sub>H<sub>3</sub>(GaCp\*)<sub>7</sub>]<sup>+</sup> fragment in [Ru<sub>2</sub>H<sub>3</sub>(Ga)(GaCp\*)<sub>7</sub>]<sup>+</sup> by the EDA-NOCV method at BP86-D3/TZ2P//PBE0/def2-SVP level. Energies are given in kcal/mol.

	Model A(Ru←Ga→Ru dative bonds)	Model B(Ru-Ga-Ru covalent bonds)	Model C(Ru→Ga←Ru dative bonds)
Interacting fragments	Ga <sup>-</sup> (singlet) + [Ru <sub>2</sub> H <sub>3</sub> (GaCp*) <sub>7</sub> ] <sup>+</sup> (singlet)	Ga <sup>+</sup> (triplet) + [Ru <sub>2</sub> H <sub>3</sub> (GaCp*) <sub>7</sub> ] <sup>-</sup> (triplet)	Ga <sup>3+</sup> (triplet) + [Ru <sub>2</sub> H <sub>3</sub> (GaCp*) <sub>7</sub> ] <sup>3-</sup> (singlet)
ΔE <sub>int</sub>	-265.2	-385.2	-1570.1
ΔE <sub>Pauli</sub>	+815.5	+293.7	+129.2
ΔE <sub>disp</sub>	-8.0	-8.0	-8.0
ΔE <sub>elstat</sub> <sup>[a]</sup>	-783.5 (73.0%)	-398.1 (59.3%)	-805.9 (47.6%)
ΔE <sub>orb</sub> <sup>[a]</sup>	-289.2 (27.0%)	-272.9 (40.7%)	-885.4 (52.4%)

[a]The percentage values in parentheses give the contribution to the total attractive interactions ΔE<sub>elstat</sub> + ΔE<sub>orb</sub>.

**Table S7.** Optimized Cartesian coordinates of stationary points for the title cluster.

Atom				
Bi		-1.40674200	1.96423300	2.16271800
Bi		-2.05043900	-1.01092700	2.01312800
Bi		1.522212100	1.90017800	2.07729200
Nb		0.00822100	2.66817400	-0.40433000
Ga		-0.01465800	0.03888500	-0.05794900
Bi		-2.09919300	1.26696900	-1.96097900
Bi		-1.87860100	-1.77642100	-1.87112000
Bi		-3.97946500	-0.38462100	-0.21438500
Bi		1.82580400	-1.78720000	-1.87143500
Nb		-0.03024500	-2.56487600	0.37291700
Bi		2.11662500	1.24817600	-1.94717700
Bi		3.98180000	-0.44696100	-0.23816200
Bi		2.04283100	-1.09109100	1.98017200
C		1.26362400	4.42497300	-1.38853200
C		0.09687800	4.15776400	-2.18833600
C		1.16958600	4.78354300	-0.04374400
C		-1.30677100	4.67813200	-0.22232100
C		-0.11361400	4.76932100	0.57386800
C		-1.16759100	4.39383800	-1.57983100
C		-1.25208500	-4.59124100	-0.01641800
C		-1.32257600	-4.37090300	1.35399000
C		-0.09975300	-4.14704200	2.07558800
C		-0.01044500	-4.58529500	-0.72695600
C		1.18739400	-4.59935100	0.06891200
C		1.15449400	-4.41986600	1.44725800
H		2.24135300	4.39109800	-1.85809000
C		0.21461300	4.02519000	-3.67721900
C		2.38072800	5.19696400	0.72918000
C		-2.64553100	4.98531700	0.36772600
H		-2.17313700	-4.73620900	-0.57247400
H		2.32122300	4.87341100	1.77184900
H		2.47118100	6.28960000	0.72634500
H		3.29231200	4.78165700	0.29529400
H		-0.19816900	5.02048000	1.62461900
C		-2.62646700	-4.48109700	2.07854000
H		-0.13554900	-4.00272500	3.14847800
C		0.03728200	-5.01317200	-2.16216800
H		-2.06300400	4.31574700	-2.19009700
H		2.14220300	-4.76110600	-0.42021400
C		2.39259000	-4.57517200	2.27093300
H		1.11580200	3.47448100	-3.95724100
H		0.26485900	5.00912700	-4.16353700
H		-0.64215100	3.49117700	-4.09476200
H		-3.44530600	4.49904900	-0.19505900
H		-2.83297700	6.06608900	0.35859600
H		-2.71002300	4.64724800	1.40550700
H		-2.64174100	-3.85909900	2.97616900
H		-2.79557600	-5.51863000	2.39114500
H		-3.46192900	-4.17770400	1.44291500
H		-0.82802600	-4.64120500	-2.71691700
H		0.04402700	-6.10796300	-2.25263100
H		0.93466800	-4.63733400	-2.66050800
H		3.29145300	-4.36580400	1.68758500
H		2.46102200	-5.60501500	2.64097200
H		2.38710900	-3.91231300	3.13920800

**Table S8.** Optimized Cartesian coordinates of stationary points for the [Ru<sub>2</sub>H<sub>3</sub>(Ga)(GaCp<sup>+</sup>)<sub>7</sub>] cluster.

Atom				
Ru		2.32135300	-0.12775900	-0.14237400
H		2.24160900	-0.35775300	-1.74649500
Ga		-0.08194900	-0.08128800	-0.09957400
Ga		1.99718000	-2.43500500	-0.28366300
Ga		1.99718000	-2.43500500	-0.28366300
Ga		2.18754700	0.20337300	2.21018000
Ru		-2.37862500	-0.26104400	0.13217200
H		-1.80384800	-1.77800400	0.16217800
H		-1.78607200	-0.28605700	1.64350400
Ga		2.12918300	2.05524700	-0.93689200
Ga		-4.32009200	-1.23325700	1.04744400
Ga		-2.85968100	-0.47767100	-2.17358100
Ga		-3.00508600	2.00055500	0.44421700
C		2.69301500	-0.31127100	4.43980200
C		2.90703600	1.08298500	4.26563200
C		1.30858100	-0.56833700	4.24653100
H		3.45565600	-1.05103200	4.68106300
C		1.65421300	1.68286000	3.96601800
H		3.86273300	1.59961100	4.34773000
C		0.66728600	0.66327700	3.95510700
H		0.82170600	-1.54134500	4.30026800
H		1.48239700	2.74068700	3.77028900
H		-0.39036200	0.79020600	3.72378700
C		2.94247800	3.80555100	-2.23541900
C		1.77373500	3.30014800	-2.86809600
C		2.55895600	4.35586700	-0.98195600
H		3.95348700	3.77486900	-2.64000600
C		0.66981800	3.53858300	-2.00734000
H		1.73418100	2.80638200	-3.83833700
C		1.15492900	4.18907200	-0.84207100
H		3.22568700	4.81966400	-0.25592700
H		-0.36235900	3.23956000	-2.18951400
H		0.55577000	4.49202300	0.01576800
C		6.67406200	-1.50311300	-0.55099300
C		6.63986500	-0.52856400	-1.58169200
C		6.79983800	-0.82607100	0.69009500
H		6.60948800	-2.58201200	-0.68819800
C		6.74514800	0.75116600	-0.97796700
H		6.54260400	-0.72792200	-2.64835500
C		6.84382500	0.56780100	0.42619000
H		6.85230600	-1.29357000	1.67281000
H		6.74663000	1.70726200	-1.50043300
H		6.93658500	1.35792400	1.17065800
C		0.43657600	-4.10557300	-0.72493500
C		1.44271100	-4.15329000	-1.72680800
C		1.04482100	-4.41482400	0.52036100
H		-0.60889500	-3.83401500	-0.87193100
C		2.67352900	-4.49610100	-1.10059000
H		1.29952200	-3.95195700	-2.78783300
C		2.42594000	-4.65872100	0.28998200
H		0.53873500	-4.44283300	1.48464000
H		3.63558700	-4.61086400	-1.59874500
H		3.16660500	-4.91757000	1.04583000
C		-1.89791500	-0.57180600	-4.38047500
C		-2.52381600	-1.82007400	-4.13341100
C		-2.90454000	0.42704400	-4.39968900

H		-0.82901600	-0.40805000	-4.51487500
C		-3.91870100	-1.59398300	-4.00283100
H		-2.02235700	-2.78415000	-4.05335900
C		-4.15435500	-0.20442700	-4.16729000
H		-2.74721000	1.49336800	-4.55971900
H		-4.67486200	-2.35308700	-3.80536700
H		-5.12383400	0.29050200	-4.11975000
C		-6.15000200	-2.77841600	0.93812000
C		-5.27938900	-3.18751700	1.98232300
C		-6.71032500	-1.52683100	1.29931700
H		-6.34691100	-3.32730700	0.01778400
C		-5.30265300	-2.18620000	2.98882600
H		-4.69472500	-4.10656100	2.00642500
C		-6.18695200	-1.16047000	2.56505700
H		-7.40986200	-0.94286300	0.70196400
H		-4.73667500	-2.20064000	3.91966900
H		-6.41498100	-0.24657300	3.11268600
C		-4.69116600	3.60696100	1.03463500
C		-3.67559900	3.66913300	2.02303300
C		-4.13270000	4.03587500	-0.19612900
H		-5.71695600	3.27464600	1.19070400
C		-2.48919700	4.13910900	1.40259400
H		-3.78473000	3.39800200	3.07259100
C		-2.77208300	4.36679800	0.03089600
H		-4.65563400	4.09573600	-1.15009200
H		-1.53078600	4.29535000	1.89715500
H		-2.07157600	4.73644800	-0.71749000

**Table S9.** Optimized Cartesian coordinates of stationary points for Bi<sub>5</sub><sup>-</sup>.

Atom				
Bi		0.00000000	2.41093500	0.00000000
Bi		1.41711200	-1.95048800	0.00000000
Bi		2.29293600	0.74502000	0.00000000
Bi		-2.29293600	0.74502000	0.00000000
Bi		-1.41711200	-1.95048800	0.00000000

**Table S10.** Optimized Cartesian coordinates of stationary points for [Bi<sub>5</sub>NbMes]<sup>-</sup>.

Atom				
Bi		1.98522300	-0.58979500	1.44513100
Bi		-0.75092100	-0.63480400	-2.34303800
Nb		-0.00804500	1.17762000	0.00000000
C		-0.73358900	3.02951500	-1.21891300
H		-1.27151200	3.01796100	-2.16004500
C		0.68477700	3.06230100	-1.23686200
C		0.68477700	3.06230100	1.23686200
C		-0.73358900	3.02951500	1.21891300
H		-1.27151200	3.01796100	2.16004500
C		1.37493800	3.07454400	0.00000000
H		2.45923100	3.07856200	0.00000000
C		1.41903000	3.18151900	2.53471400
H		0.89769300	2.63589300	3.32447900
H		1.49757800	4.23306200	2.84002100
H		2.42647500	2.76821500	2.45613000
C		-1.46357800	3.01977100	0.00000000
C		1.41903000	3.18151900	-2.53471400
H		2.42647500	2.76821500	-2.45613000
H		1.49757800	4.23306200	-2.84002100
H		0.89769300	2.63589300	-3.32447900
C		-2.95257000	3.17937900	0.00000000

H		-3.39902800	2.71579000	-0.88143600
H		-3.22333500	4.24405700	0.00000000
H		-3.39902800	2.71579000	0.88143600
Bi		1.98522300	-0.58979500	-1.44513100
Bi		-0.75092100	-0.63480400	2.34303800
Bi		-2.43732400	-0.60223700	0.00000000

**Table S11.** Optimized Cartesian coordinates of stationary points for  $[\text{Bi}_5\text{Nb}_2\text{Mes}_2]^-$ .

Atom				
Bi		-2.45257000	-0.00067100	0.78111300
Bi		2.45257000	0.00067100	0.78111300
Nb		0.00000000	1.52522800	-0.00210000
Nb		0.00000000	-1.52522800	-0.00210000
C		0.97895200	-3.44416700	1.00716000
H		1.73667100	-3.43647700	1.78094100
C		1.36009600	3.42164200	0.34853100
H		2.40873100	3.43385400	0.61766400
C		0.38507300	3.43625700	1.37697500
C		-1.36009600	-3.42164200	0.34853100
H		-2.40873100	-3.43385400	0.61766400
C		0.38201400	-3.44429600	-1.34707700
H		0.68053100	-3.45449500	-2.38811900
C		-1.37970700	3.46040400	-0.34668500
C		1.37970700	-3.46040400	-0.34668500
C		-0.38201400	3.44429600	-1.34707700
H		-0.68053100	3.45449500	-2.38811900
C		-0.97895200	3.44416700	1.00716000
H		-1.73667100	3.43647700	1.78094100
C		2.82297600	-3.57397300	-0.71722300
H		3.02161800	-3.07232600	-1.66685800
H		3.11266700	-4.62778500	-0.81702300
H		3.45979400	-3.11216000	0.04038500
C		-0.99580600	-3.43882700	-1.02084900
C		-2.82297600	3.57397300	-0.71722300
H		-3.02161800	3.07232600	-1.66685800
H		-3.11266700	4.62778500	-0.81702300
H		-3.45979400	3.11216000	0.04038500
C		0.99580600	3.43882700	-1.02084900
C		-0.80519500	-3.58309300	2.80415400
H		-0.04193000	-3.19876600	3.48303300
H		-0.98253700	-4.63954800	3.04548300
H		-1.72844300	-3.03105400	2.99492000
C		0.80519500	3.58309300	2.80415400
H		0.04193000	3.19876600	3.48303300
H		0.98253700	4.63954800	3.04548300
H		1.72844300	3.03105400	2.99492000
C		-0.38507300	-3.43625700	1.37697500
C		-2.03873600	-3.62046400	-2.07769600
H		-2.96087500	-3.09822100	-1.81439300
H		-2.27377400	-4.68614900	-2.20188100
H		-1.69953500	-3.23187600	-3.03941800
C		2.03873600	3.62046400	-2.07769600
H		2.96087500	3.09822100	-1.81439300
H		2.27377400	4.68614900	-2.20188100
H		1.69953500	3.23187600	-3.03941800
Bi		0.00000000	0.00000000	2.51801400
Bi		-1.51405700	0.00628100	-2.04147400
Bi		1.51405700	0.00628100	-2.04147400

## References

- [1] C. Fausto, P. Guido, R. Lucia, S. Joachim, W. Klaus, *J. Organomet. Chem.* **1991**, *413*, 91-109.
- [2] G. M. Sheldrick, *Acta Crystallogr. Sect. A: Found. Adv.* **2015**, *71*, 3-8.
- [3] O. V. Dolomanov, L. J. Bourhis, R. J. Gildea, J. A. K. Howard, H. Puschmann, *J. Appl. Crystallogr.* **2009**, *42*, 339-341.
- [4] A. L. Spek, *Acta Crystallogr., Sect. D: Biol. Crystallogr.* **2009**, *65*, 148-155.
- [5] A. L. Spek, *Acta Crystallogr. Sect. C Cryst. Struct. Commun.* **2015**, *71*, 9-18.
- [6] M. J. Frisch, G. W. Trucks, H. B. Schlegel, G. E. Scuseria, M. A. Robb, J. R. Cheeseman, G. Scalmani, V. Barone, B. Mennucci, G. A. Petersson, H. Nakatsuji, M. Caricato, X. Li, H. P. Hratchian, A. F. Izmaylov, J. Bloino, G. Zheng, J. L. Sonnenberg, M. Hada, M. Ehara, K. Toyota, R. Fukuda, J. Hasegawa, M. Ishida, T. Nakajima, Y. Honda, O. Kitao, H. Nakai, T. Vreven, J. A. Montgomery Jr., J. E. Peralta, F. Ogliaro, M. Bearpark, J. J. Heyd, E. Brothers, K. N. Kudin, V. N. Staroverov, R. Kobayashi, J. Normand, K. Raghavachari, A. Rendell, J. C. Burant, S. S. Iyengar, J. Tomasi, M. Cossi, N. Rega, J. M. Millam, M. Klene, J. E. Knox, J. B. Cross, V. Bakken, C. Adamo, J. Jaramillo, R. Gomperts, R. E. Stratmann, O. Yazyev, A. J. Austin, R. Cammi, C. Pomelli, J. W. Ochterski, R. L. Martin, K. Morokuma, V. G. Zakrzewski, G. A. Voth, P. Salvador, J. J. Dannenberg, S. Dapprich, A. D. Daniels, Ö. Farkas, J. B. Foresman, J. V. Ortiz, J. Cioslowski and D. J. Fox, *GAUSSIAN 09W* (Revision A.1), Gaussian Inc., Wallingford, CT, 2010.
- [7] E. D. Glendening, J. K. Badenhoop, A. E. Reed, J. E. Carpenter, J. A. Bohmann, C. M. Morales, C. R. Landis, F. Weinhold, NBO 6.0.; Theoretical Chemistry Institute, University of Wisconsin:Madison, 2013.
- [8] E. J. Baerends , T. Ziegler , A. J. Atkins , J. Autschbach , O. Baseggio , D. Bashford , A. Bérces , F. M. Bickelhaupt , C. Bo , P. M. Boerrigter , L. Cavallo , C. Daul , D. P. Chong , D. V. Chulhai , L. Deng , R. M. Dickson , J. M. Dieterich , D. E. Ellis , M. van Faassen , L. Fan , T. H. Fischer , A. Förster , C. Fonseca Guerra , M. Franchini , A. Ghysels , A. Giammona , S. J. A. van Gisbergen , A. Goez , A. W. Götz , J. A. Groeneveld , O. V. Gritsenko , M. Grüning , S. Gusarov , F. E. Harris , P. van den Hoek , Z. Hu , C. R. Jacob , H. Jacobsen , L. Jensen , L. Joubert , J. W. Kaminski , G. van Kessel , C. König , F. Kootstra , A. Kovalenko , M. V. Krykunov , E. van Lenthe , D. A. McCormack , A. Michalak , M. Mitoraj , S. M. Morton , J. Neugebauer , V. P. Nicu , L. Noddleman , V. P. Osinga , S. Patchkovskii , M. Pavanello , C. A. Peebles , P. H. T. Philipsen , D. Post , C. C. Pye , H. Ramanantoanina , P. Ramos , W. Ravenek , J. I. Rodríguez , P. Ros , R. Rüger , P. R. T. Schipper , D. Schlüns , H. van Schoot , G. Schreckenbach , J. S. Seldenthuis , M. Seth , J. G. Snijders , M. Solà , M. Stener , M. Swart , D. Swerhone , V. Tognetti , G. te Velde , P. Vernooyjs , L. Versluis , L. Vischer , O. Visser , F. Wang , T. A. Wesolowski , E. M. van Wezenbeek , G. Wiesenecker , S. K. Wolff , T. K. Woo and A. L. Yakovlev , S. ADF 2019.3, SCM, Theoretical Chemistry , Vrije Universiteit, Amsterdam, The Netherlands, 2019.
- [9] J. P. Perdew, K. Burke, M. Ernzerhof, *Phys. Rev. Lett.* **1996**, *77*, 3865–3868.
- [10] C. Adamo; B. Vincenzo, *J. Chem. Phys.* **1999**, *110*, 6158–6170.
- [11] A. Schaefer, H. Horn, R. Ahlrichs, *J. Chem. Phys.* **1992**, *97*, 2571-2577.
- [12] J. Tomasi, B. Mennucci, R. Cammi, *Chem. Rev.* **2005**, *105*, 2999-3094.
- [13] S. F. Boys, *Rev. Mod. Phys.* **1960**, *32*, 296-299;
- [14] J. M. Foster, S. F. Boys, *Rev. Mod. Phys.* **1960**, *32*, 300-302.
- [15] T. Lu, F. W. Chen, *J. Comp. Chem.* **2012**, *33*, 580-592.
- [16] W. Humphrey, A. Dalke, K. Schulten, *J. Mol. Graph.* **1996**, *14*, 33-38.
- [17] R. F. W. Bader, *Atoms in Molecules: A Quantum Theory* (Clarendon Press, 1990).
- [18] T. Ziegler, A. Rauk, *Theor. Chim. Acta* **1977**, *46*, 1-10.
- [19] M. Mitoraj, A. Michalak, *J. Mol. Model.* **2008**, *14*, 681-687.
- [20] M. P. Mitoraj, A. Michalak, T. Ziegler, *J. Chem. Theory Comput.* **2009**, *5*, 962-975.
- [21] A. D. Becke, *Phys. Rev. A* **1988**, *38*, 3098-3100.
- [22] J. P. Perdew, *Phys. Rev. B* **1986**, *33*, 8822-8824.
- [23] S. Grimme, S. Ehrlich, L. Goerigk, *J. Comput. Chem.* **2011**, *32*, 1456-1465.
- [24] E. Van Lenthe, E. J. Baerends, *J. Comput. Chem.* **2003**, *24*, 1142-1156.
- [25] L.-L. Zhao, S. Pan, N. Holzmann, P. Schwerdtfeger, G. Frenking, *Chem. Rev.* **2019**, *119*, 8781-8845.
- [26] L.-L. Zhao, M. Hermann, W. H. Eugen Schwarz, G. Frenking, *Nat. Rev. Chem.* **2019**, *3*, 48-63.
- [27] D. Liu, S. Xu, G. Pei, J.-Z. Xu, X.-T. Zhao, C.-C. Kong, Z.-M. Yang, T. Yang, *J. Comput. Chem.* **2022**, *43*, 828-838;
- [28] X.-T. Zhao, G.-R. Pei, S. Xu, C.-C. Kong, Z.-M. Yang, T. Yang, *Phys. Chem. Chem. Phys.* **2021**, *23*, 20654-20665.